Supersaturation-Dependent Surface Structure Evolution: From Ionic, Molecular to Metallic Micro/Nanocrystals

Hai-xin Lin, Zhi-chao Lei, Zhi-yuan Jiang, Chang-ping Hou, De-yu Liu, Min-min Xu, Zhong-qun Tian,* and Zhao-xiong Xie*

State Key Laboratory of Physical Chemistry of Solid Surfaces and College of Chemistry and Chemical Engineering, Xiamen University, Xiamen 361005, China

S *Supporting Information*

ABSTRACT: Deduced from thermodynamics and the Thomson−Gibbs equation that the surface energy of crystal face is in proportion to the supersaturation of crystal growth units during the crystal growth, we propose that the exposed crystal faces can be simply tuned by controlling the supersaturation, and higher supersaturation will result in the formation of crystallites with higher surface-energy faces. We have successfully applied it for the growth of ionic (NaCl), molecular (TBPe), and metallic (Au, Pd) micro/nanocrystals with high-surface-energy faces. The above proposed strategy can be rationally designed to synthesize micro/nanocrystals with specific crystal faces and functionality toward specific applications.

Crystals with different faces exposed usually exhibit different physical and chemical properties due to its anisotropic property, one of the basic properties of crystals.[1−6] In nature, however, crystals tend to expose the most stable faces. To study the surface structure-dependent properties, such as many studies concerning surface science, the specific crystal face was achieved by oriented cutting or polishing of macrocrystal. However, in many applied fields, such as catalysis, crystals in micro/nano level are required, rendering the above techniques inapplicable to achieve specific crystal faces. Instead, control of the exposed faces during crystal growth is the best way. Theoretically, crystal faces can be chemically fabricated either by thermodynamically reducing surface energy via selective adsorption of capping agents on specific crystal faces[7−9] or delicate control over the growth kinetics.[10−15] Despite prolonged effects in the past decade, it is still extremely difficult to predict or design the surface structure of micro/nanocrystals. A general method to control the exposed crystal face is needed.

Herein, from thermodynamics and the well-known Thomson−Gibbs equation,[16] we reason that the surface of crystals can be easily controlled via simply adjusting supersaturation of crystal growth units in the growth medium during the crystal growth process. The crystal faces with higher surface energy will appear when the supersaturation of the growth units is increased in the medium. Such inference combines both apparent thermodynamic and kinetic factors that governs the crystal growth process, and has been successfully validated by examples ranging from ionic, molecular to metallic crystals. The proposed supersaturation strategy provides an effective way to control the shape and surface structures of micro/nanocrystals, which is important for both fundamental research and practical applications.[17,18]

As is well-known, higher supersaturation results in smaller crystallites during the crystallization. This phenomenon was well explained by the Thomson−Gibbs equation[16] as shown below:

$$\Delta\mu = \mu_1 - \mu_c = \frac{2\sigma v}{h} \tag{1}$$

where μ_1 and μ_c are the chemical potentials of solute in solution and solid crystal respectively, and their difference $\Delta\mu$ is the supersaturation (see S1.1 for the relationship between chemical potential and supersaturation), σ is the specific surface energy of crystallite, v is the volume of single building block, and h is the distance from the center to the surface of the crystallite (the size of crystallites). In fact, the Thomson−Gibbs equation was originated from thermodynamics equilibrium. Considering the case of constant pressure P and temperature T ($dP = dT = 0$), the variation of Gibbs free energy G (P, T, n_1, n_c, S) of the crystallization system gives

$$\Delta G = \mu_1 dn_1 + \mu_c dn_c + \sigma dS = 0 \tag{2}$$

where S is the surface area of crystallites, n_1 and n_c are the number of moles of crystal building block in solution and crystal phases, respectively.[16] Then it is very easy to deduce the Thomson−Gibbs equation $\Delta\mu = \mu_1 - \mu_c = (2\sigma v/h)$ (detailed deduction can be found in S1.2). From eq 2, it can be found that that when crystallization occurred, the excessive energy (the difference between $\mu_1 dn_1$ and $\mu_c dn_c$) should convert to surface energy of crystallites (σdS) in the ideal case of constant pressure and temperature because of the conservation of energy. Therefore, when crystallizing from a supersaturated solution, the number of crystallites usually increases, and the size of crystallites usually decreases with the increase of supersaturation in order to increase the total surface energy of crystallites for an equilibrium system (mainly governed by nucleation process).

For crystal growth process, similarly, the excessive energy for transforming the solute into crystal should be transferred to surface energy of crystallites (in ideal case of constant pressure and temperature). If nucleation does not occur (no new nucleus forms) during the crystal growth under a supersaturated condition (not under an equilibrium condition), the surface energy of crystallites should increase with the increase of supersaturation. Therefore, beyond the influence of well-known

factors, such as capping effect, the supersaturation should further affect the surface energy and thus determines the surface structures of the crystals. By simply adjusting the supersaturation during the crystal growth, we could control the shape and the surface structures of micro/nanocrystals to some extent. The crystal faces with higher surface energy will appear when the supersaturation of the growth units increases during the crystal growth.

The supposition was first examined for ionic crystal NaCl, whose crystal structure can be represented as a face-centered cubic (fcc) lattice, with the electrostatic force as the dominating force between the building blocks. In such a crystal, the surface energy of {100} faces is the lowest, and the surface energy of {110} surfaces is higher than that of {100} surfaces (Figure S1).[19] That is why the ordinary NaCl crystallites have cube shapes with {100} faces exposed.

The highly polar solvents, such as H_2O and CH_3OH, are good solvents for NaCl, which can dissolve NaCl well because of the stronger electrostatic interaction between the solvent and the solute. In such solvents, if crystal growth of NaCl is carried out by slow evaporation, the supersaturation is usually very low, and thus cube crystallites with {100} faces are formed (Figure 1a).
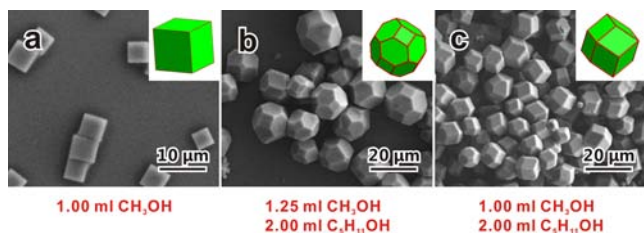

Figure 1. Typical SEM images of as prepared NaCl microcrystals. (a) Cubic NaCl microcrystals prepared by slowly evaporating methanol from NaCl-methanol solutions. (b) NaCl truncated RD prepared in the mixture of 1.25 mL methanol and 2.0 mL *n*-pentanol. (c) NaCl RD prepared in the mixture of 1.00 mL methanol and 2.0 mL *n*-pentanol.

However, adding these NaCl solutions into less polar solvent (such as *n*-pentanol, poor solvent) quickly will rapidly decrease the solubility of NaCl and increase its supersaturation (see S1.3 for details). According to our supposition, high-energy surfaces will appear in this case. In fact, the shapes of NaCl microcrystals change to truncated rhombic dodecahedron (Figure 1b) and then rhombic dodecahedron (RD, Figure 1c) when NaCl crystal was respectively grown by injecting NaCl-methanol (good solvent) solution rapidly into a mixture of *n*-pentanol and methanol (poor solvent) solution by decreasing the portion of methanol. It should be noted, in such a case, high supersaturation status can be kept not only in the stage of nucleation but also in the stage to crystal growth, due to continuous diffusion of *n*-pentanol into NaCl-methanol solution. A truncated RD is enclosed by 12 {110} and 6 {100} faces, whereas an RD is enclosed by 12 {110} faces with higher surface energy. Therefore, these observations prove that the increasing super-saturation of growth units during the crystal growth will result in the formation of crystal faces of higher surface energy.

The above observation was further corroborated using an organic molecular crystal, 2,5,8,11-tetra-*tert*-butylperylene (TBPe). The TBPe crystal adopts body-centered cubic (bcc) structure, and van der Waals forces among the TBPe molecules are the main interaction force between the building blocks. For such a bcc structure, the {110} faces are of lowest surface energy, and the surface energy of {100} face is higher than that of {110}

(Figure S2). TBPe is more soluble in less polar solvents as there are no hydrophilic groups in its molecule. It can be expected that adding of TBPe solution into a polar solvent would result in higher supersaturation condition and thus leading to the appearance of TBPe crystals with high energy faces. We then chose THF as good solvent and water as the poor solvent according to the previous report.[20] As showed in Figure 2, TBPe
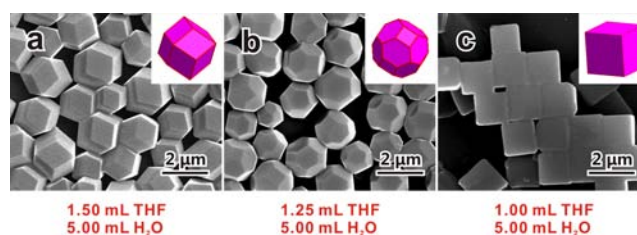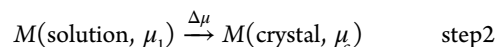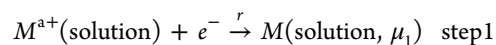

Figure 2. Typical SEM images of TBPe microcrystals prepared in the different solution. (a) TBPe RD crystals. (b) Truncated RD TBPe crystals. (c) TBPe cubes.

RD crystals (Figure 2a) are achieved in high ratio of THF to H_2O, then the truncated RD crystals (Figure 2b) appear with decreased THF portion. And finally TBPe cubes (Figure 2c) with high-energy surfaces {100} are achieved. These results confirm that the increase of supersaturation by adding the growth solution in poor solvent will result in an increase of surface energy of exposed crystal faces.

Encouraged by the success of controlling the surfaces of ionic and molecular crystals, the supersaturation-based strategy was extended to synthesize shape controlled metallic nanocrystals, where the metallic bond is the main interaction between the building blocks. Herein, Au nanocrystals were employed as a model system due to its chemical and structural stability.[21,22] For Au nanocrystals with an fcc structure, the specific surface energies of different crystal faces are in the sequence of $\sigma_{111} < \sigma_{100} < \sigma_{331} < \sigma_{110}$ (Figure S3). Being different from NaCl and TBPe, the reduction reaction is indispensable for growing Au nanocrystals via solution chemistry strategy. The growth process of Au nanocrystals can be described as following:

$$M^{a+}(\text{solution}) + e^- \xrightarrow{r} M(\text{solution}, \mu_1) \quad \text{step1}$$

$$M(\text{solution}, \mu_1) \xrightarrow{\Delta\mu} M(\text{crystal}, \mu_c) \qquad \text{step2}$$

where r is the reduction reaction rate of metal (Au) precursor (M^{a+}), $\Delta\mu$ is the supersaturation of the metal crystal growth units. The metal precursor should be first reduced to the metallic atoms (step 1), and then the metallic atoms grow on the crystallites (step 2), which is driven by the supersaturation.

From the above equations, it is easy to understand that the chemical potential of reduced metallic atoms in solution (μ_1) will increase with the increasing metal reduction rate (r). The supersaturation ($\Delta\mu$) of metal atoms, i.e., the difference of chemical potentials of metal atoms between solution phase (μ_1) and solid phase (μ_c), will increase with the increase of metal reduction rate. One can expect that with the increasing reduction rate, the supersaturation should increase, and the exposed crystal faces should evolve from low surface energy {111} to higher energy surfaces, such as {100}, {331}, and {110}. It should be noted the formation of nanocrystals usually includes nucleation and crystal growth steps. The nucleation step greatly disturbs the supersaturation. To avoid the change of supersaturation during nucleation process (in our proposed strategy, it is very important

to keep high supersaturation during the crystal growth process), seed-mediated growth was then designed to investigate the correlation among the reduction rate of Au precursors and the ultimate shape/surface structures of the Au nanocrystals.

Under the reaction condition with a constant and large excess of reductant ascorbic acid (AA), the reduction reaction rate is proportional to the concentration of Au precursors. Thus, we controlled the reduction rate by varying the concentration of Au precursors and used small octahedron (Figure S4) as the seed to avoid the nucleation. As shown in Figure 3a, with the increase of
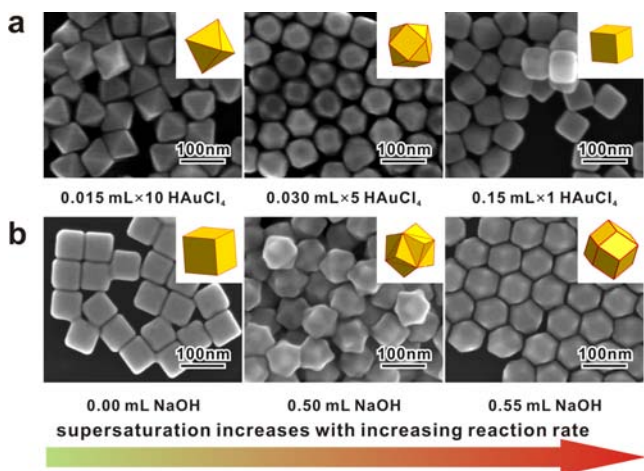

Figure 3. Typical SEM images of Au nanocrystals prepared by seed-mediated growth. (a) Au nanocrystals grew from octahedron seeds by adding the same amount of HAuCl$_4$ in the growth solutions with different feeding way. (b) Au nanocrystals grew from cube seeds by adding different volume of NaOH in the growth solution.

the concentration of Au precursors in the growth solution, the products varied from octahedral shape with {111} surfaces to cuboctahedral shape with both {111} and {100} faces, and finally to cubic shape with {100} faces. This sequence indicates accurately that a slow reduction reaction rate leads to low supersaturation and results in the formation of {111} faces, which has the lowest surface energy; while faster reduction rate leads to higher supersaturation and forms the {100} faces of higher surface energy.

Besides the concentration of Au precursors, the reduction reaction rate can be further tuned by many other parameters. For example, the increase of pH value should accelerate the reduction rate of HAuCl$_4$ dramatically because of the increase of the reducing ability of AA, which can be confirmed by UV−vis spectroscopy (Figure S5). In order to further increase the growth rate for achieving the prepared Au nanocrystals enclosed by surfaces with higher surface energy than {100} surfaces, the pH value of the solution was adjusted by adding NaOH solution. As shown in Figure 3b, the morphologies of Au nanocrystals evolve from cube to trioctahedron (TOH) and then to RD with increasing amounts of NaOH. The exposed crystal faces are {100} for cube, {331} for TOH, and {110} for RD (Figures S6−S7). Similar evolution phenomenon can also be observed by controlling the growth rates via adjusting other parameters, such as the concentration of reducing agent (Figure S8). These results confirm that higher supersaturation leads to the formation of crystal faces with higher surface energies. It should be mentioned that supersaturation can not be infinitely increased because secondary nucleation will start to occur when the superaturation is high enough to reach the critical value of nucleation (Figure

S9). The occurrence of secondary nucleation by increasing the reduction rate to a certain value is also a powerful evidence to confirm that supersaturation is related to the reaction rate in the present case.

It should be noted that the above experiments were carried out in a set of similar conditions for the growth of Au nanocubes reported previously, using CTAB as capping agents. From previous viewpoints, CTAB was considered as surface stabilizer to change the surface energy sequence of crystal faces to induce the formation of {100} faces. Therefore, higher concentration ratio of the surfactant CTAB to Au precursor would result in the formation of larger {100} faces. However, in our experiment, Au octahedra with {111} faces were achieved in high-concentration ratio of CTAB to Au precursor (left of Figure 3); while Au cubes with {100} faces were obtained at low-concentration ratio of CTAB to Au precursor (right of Figure 3). In addition, {111}, {100}, {331}, {110} faces can all be formed in the same concentration of CTAB by simply varying the reduction rate.

The above results indicate that there is no direct relationship between the surfactant CTAB and the specific surface structure of gold nanocrystals. The surfactant CTAB is not the key factor for the formation of specific face (e.g., high index (311) face). Therefore, the result cannot be explained by the capping agent effect of CTAB but can be inferred by our proposed supersaturation effect obviously. It can be concluded that beyond the tuning of the surface energies of crystal faces by the adsorption of capping agents, the supersaturation (determining growth rate in most case) should further tune the surface energy of crystal faces, which provide a powerful way to design and prepare functional nanocrystals with desired crystal faces of high surface energy.

The proposed strategy can also be employed to synthesize other metal nanocrystals. As a well-known noble metal, palladium plays a key role in many industrial applications. Although many attempts have been carried out to control the surface structures and crystal morphologies, only few examples[23,24] concerned Pd nanocrystals with high-index (high surface energy) surfaces. Based on our proposed supersaturation strategy, it is believed that Pd nanocrystals with high-index surface can be synthesized by simply increasing the reduction rate. It has been known the capping agent, such as CTAC or CTAB, would affect the reduction and crystal growth rate of metals like Au and Pd, and the reaction and crystal growth rate would increase with decreasing concentration of capping agent or halide ions.[15,23,24] Therefore, Pd nanocrystals with high index faces could be prepared by simply decreasing or removal of the capping agent.

Figure 4 shows the Pd nanocrystals prepared in the presence or absence of CTAC (see S2.7). As shown in Figure 4a, the Pd nanocubes were prepared in the presence of capping agent CTAC. When we directly reduce H$_2$PdCl$_4$ by AA without adding any capping agent, the products were dominated with tetrahexahedral (THH) shape as shown in Figure 4b. The crystal surfaces were high index {730} faces, analyzed by the TEM image, corresponding SAED pattern and an ideal THH model surrounded by {730} faces, as shown in Figure 4c,d. The results indicate that neither CTA ion nor halide ion play key role in the formation of high-energy face in some conditions, and the supersaturation is the key to determine the surface structures.

In addition to the above experiment facts, the proposed supposition can also be principally verified by the results reported in the literature.[23−29] For example, it was found very recently that the reduction rate, which can be can be affected by pH,
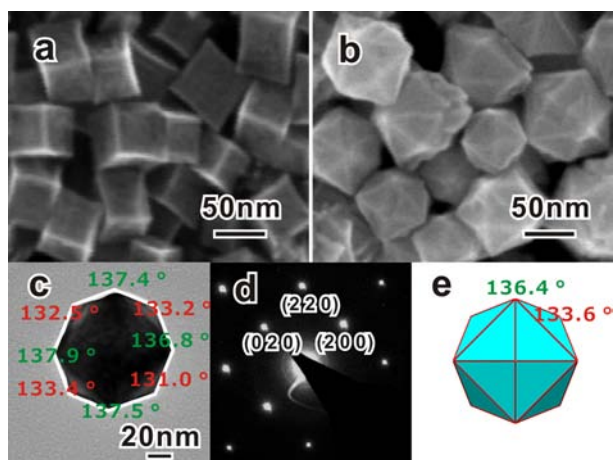
Figure 4. Typical morphology and structure features of Pd nanocrystals prepared via reducing H$_2$PdCl$_4$ by AA. (a) Pd cubes synthesized in CTAC-water solution. (b) Pd THH synthesized without CTAC. (c) TEM image and (d) corresponding SAED patterns of an individual Pd THH; (e) ideal model of THH surrounded by {730} faces projected along [001] direction.

concentration, complex reaction, temperature and so on, will affect crystal shape and surface structure.[11,12,14,15,28] However, it is difficult to understand why the faster reduction rate results in the higher surface energy of crystallites. It seems difficult to be simply attributed to "kinetics effect". Considering the fact that the supersaturation is the driving force for the crystal growth, and faster reduction rate would result in higher supersaturation and crystal faces with higher surface energies, many recent reported results can be well explained (detailed discussions in S5).

In summary, inspired from thermodynamics and the Thomson–Gibbs equation, we understand crystal growth from a new viewpoint and deduce that the surface energy of crystal faces is related to the supersaturation of the growth units during the crystal growth. When other factors are the same, the supersaturation can be a key factor to decide the exposed facets of crystals. The proposed strategy, which has been successfully validated by examples ranging from ionic, molecular to metallic crystals, provides a general way to tune the surface energy of micro/nanocrystals. In addition, the proposed mechanism provides a deep insight into how apparent kinetic parameters such as growth rate of crystals affects the surface energy of crystal faces, a thermodynamic quantity. It is believed that micro/nanocrystals with specific crystal faces and functionality can be rationally designed and realized by the proposed strategy.

ASSOCIATED CONTENT

S Supporting Information

Experimental details and characterization data. This material is available free of charge via the Internet at http://pubs.acs.org.

AUTHOR INFORMATION

Corresponding Author

zxxie@xmu.edu.cn; zqtian@xmu.edu.cn

Notes

The authors declare no competing financial interest.

ACKNOWLEDGMENTS

REFERENCES

(1) Xie, X. W.; Li, Y.; Liu, Z. Q.; Haruta, M.; Shen, W. J. *Nature* **2009**, *458*, 746.

(2) Tian, N.; Zhou, Z. Y.; Sun, S. G.; Ding, Y.; Wang, Z. L. *Science* **2007**, *316*, 732.

(3) Yang, H. G.; Sun, C. H.; Qiao, S. Z.; Zou, J.; Liu, G.; Smith, S. C.; Cheng, H. M.; Lu, G. Q. *Nature* **2008**, *453*, 638.

(4) Han, X. G.; Kuang, Q.; Jin, M. S.; Xie, Z. X.; Zheng, L. S. *J. Am. Chem. Soc.* **2009**, *131*, 3152.

(5) Han, X. G.; Jin, M. S.; Xie, S. F.; Kuang, Q.; Jiang, Z. Y.; Jiang, Y. Q.; Xie, Z. X.; Zheng, L. S. *Angew. Chem., Int. Ed.* **2009**, *48*, 9180.

(6) Zhang, L.; Niu, W. X.; Xu, G. B. *Nano Today* **2012**, *7*, 586.

(7) Chiu, C. Y.; Li, Y. J.; Ruan, L. Y.; Ye, X. C.; Murray, C. B.; Huang, Y. *Nat. Chem.* **2011**, *3*, 393.

(8) Xiong, Y.; Xia, Y. *Adv. Mater.* **2007**, *19*, 3385.

(9) Chen, M.; Wu, B.; Yang, J.; Zheng, N. *Adv. Mater.* **2012**, *24*, 862.

(10) Barnard, A. S.; Chen, Y. *J. Mater. Chem.* **2011**, *21*, 12239.

(11) Kang, L.; Fu, H.; Cao, X.; Shi, Q.; Yao, J. *J. Am. Chem. Soc.* **2011**, *133*, 1895.

(12) Niu, W. X.; Zheng, S. L.; Wang, D. W.; Liu, X. Q.; Li, H. J.; Han, S. A.; Chen, J.; Tang, Z. Y.; Xu, G. B. *J. Am. Chem. Soc.* **2009**, *131*, 697.

(13) Yang, C. W.; Chanda, K.; Lin, P. H.; Wang, Y. N.; Liao, C. W.; Huang, M. H. *J. Am. Chem. Soc.* **2011**, *133*, 19993.

(14) Hong, J. W.; Lee, S. U.; Lee, Y. W.; Han, S. W. *J. Am. Chem. Soc.* **2012**, *134*, 4565.

(15) Langille, M. R.; Personick, M. L.; Zhang, J.; Mirkin, C. A. *J. Am. Chem. Soc.* **2012**, *134*, 14542.

(16) Markov, I. V. *Crystal Growth for Beginners: Fundamentals of Nucleation, Crystal Growth and Epitaxy*; 2nd ed.; World Scientific: Singapore; River Edge, N.J., 2003.

(17) Jiang, Z. Y.; Kuang, Q.; Xie, Z. X.; Zheng, L. S. *Adv. Funct. Mater.* **2010**, *20*, 3634.

(18) Zhou, Z. Y.; Tian, N.; Li, J. T.; Broadwell, I.; Sun, S. G. *Chem. Soc. Rev.* **2011**, *40*, 4167.

(19) van Zeggeren, F.; Benson, G. C. *J. Chem. Phys.* **1957**, *26*, 1077.

(20) Zhang, X. J.; Dong, C.; Zapien, J. A.; Ismathullakhan, S.; Kang, Z. H.; Jie, J. S.; Zhang, X. H.; Chang, J. C.; Lee, C. S.; Lee, S. T. *Angew. Chem., Int. Ed.* **2009**, *48*, 9121.

(21) Eustis, S.; El-Sayed, M. A. *Chem. Soc. Rev.* **2006**, *35*, 209.

(22) Grzelczak, M.; Pérez-Juste, J.; Mulvaney, P.; Liz-Marzán, L. M. *Chem. Soc. Rev.* **2008**, *37*, 1783.

(23) Zhang, J. W.; Zhang, L.; Xie, S. F.; Kuang, Q.; Han, X. G.; Xie, Z. X.; Zheng, L. S. *Chem.—Eur. J.* **2011**, *17*, 9915.

(24) Jin, M. S.; Zhang, H.; Xie, Z. X.; Xia, Y. N. *Angew. Chem., Int. Ed.* **2011**, *50*, 7850.

(25) Wu, H.-L.; Kuo, C.-H.; Huang, M. H. *Langmuir* **2010**, *26*, 12307.

(26) Chen, Y. X.; Chen, S. P.; Zhou, Z. Y.; Tian, N.; Jiang, Y. X.; Sun, S. G.; Ding, Y.; Wang, Z. L. *J. Am. Chem. Soc.* **2009**, *131*, 10860.

(27) DeSantis, C. J.; Sue, A. C.; Bower, M. M.; Skrabalak, S. E. *ACS Nano* **2012**, *6*, 2617.

(28) Zhang, J.; Langille, M. R.; Mirkin, C. A. *J. Am. Chem. Soc.* **2010**, *132*, 12502.

(29) Lu, C. L.; Prasad, K. S.; Wu, H. L.; Ho, J. A. A.; Huang, M. H. *J. Am. Chem. Soc.* **2010**, *132*, 14546.